RSC Advances

ROYAL SOCIETY
OF **CHEMISTRY**

www.rsc.org/advances

RSC Advances

ARTICLE

A sensitive electrochemical sensor for the determination of carvedilol based on modified glassy carbon electrode with an ordered mesoporous carbon

Mohammad Kazem Rofouei,*[a], Hamid Khoshsafar[a], Roozbeh Javad Kalbasi[a] and Hasan Bagheri[b]

This work describes the incorporation of ordered mesoporous carbon (OMC) as a sensing material for carvedilol (CAR) detection on glassy carbon electrode (GCE). The physicochemical properties of prepared OMC as the modifier layer on GCE was studied by X-ray diffraction spectroscopy (XRD), N_2 adsorption-desorption and scanning electron microscopy (SEM) techniques. The effective surface area for OMC/GCE enhanced compared with bare GCE. The electrochemical sensor was sensitive to CAR in the range of 0.1-23.0 μmol L^{-1} with detection limit of 0.034 μmol L^{-1}. Also the effect of some interfering compounds such as glucose, lactose, glycine, valine and others, on the determination of CAR was studied, which none of them had a significant effect on the assay recovery. Moreover, its practical applicability was reliable, which is desirable for analysis of biological fluids and pharmaceutical samples.

1. Introduction

Cardiovascular disease is a leading cause of death worldwide. Carvedilol ((2RS)-1-(9H-carbazol-4-yloxy)-3-[[2-(2-methoxyphenoxy)ethyl]amino]propan-2-ol is a non-selective β-blocker with α1-adrenergicreceptor antagonism properties. It is unique among β-blockers because in addition to improving exercise, tolerance and its anti-ischemic properties secondary to a reduction in heart rate and myocardial contractility, carvedilol (CAR) exerts other beneficial effects including: antioxidant effects; neutrophil infiltration reduction; apoptosis inhibition; reduction of vascular smooth muscle migration and improvement of myocardial remodeling post-AMI. These properties are consistent with established evidence demonstrating decreased morbidity and mortality in related patients [1-3].

Co-administered medications that induce or inhibit the metabolize of CAR may alter their respective plasma concentrations, which may in turn impact the safety and efficacy of CAR [4-6]. Therefore, the development of a simple, sensitive, rapid and reliable method for the determination of CAR in clinical assays and quality controlling is of great importance. One of the most efficient approaches in this field is the use of electrochemical sensors. Electrochemical methods offer the practical advantages including operation simplicity, satisfactory sensitivity, wide linear concentration range, low expense of instrument, possibility of miniaturization, suitability for real-time detection and less sensitivity to matrix effects in comparison with separation and spectral methods [7]. However, the fabrication of sensing layer and its performance improvement is crucial in electrochemical sensors.

In order to improve the performance and enhancing the sensitivity, selectivity, limit of detection (LOD), and signal to noise ratio of electrochemical sensors, recent researches have been focused on preparation and using of chemically modified electrochemical sensors with new recognition elements instead of bare ones [8, 9]. Chemically modified matrices should possess a high conductivity and preferably low electron transfer resistance on their selective surface. Furthermore, it is also beneficial if there is a large surface area for interacting of target species. For these reasons, there is an emerging interest in nano-scale carbon materials to be used in voltammetric determination [10, 11].

As one of novel carbon materials, OMC is a kind of 3-D nanostructured porous materials which has attracted enormous interest since it was first synthesized by Ryoo et al [12]. Compared to multiwall carbon nanotubes [13, 14] and ordered mesoporous silica [15] OMC has better electrocatalytic and electrochemical properties because of its unique high surface area, periodically arranged mono-dispersed mesopore space, tunable pore sizes, alternative pore shapes, remarkable π-

[a.] Faculty of Chemistry, Kharazmi University, Tehran, Iran. E-mail address: rofouei@khu.ac.ir
[b.] Chemical Injuries Research Center, Baqiyatallah University of Medical Sciences, Tehran, Iran.

conjunction, uniform nanosized frameworks and abundant compositions [16] These merits lead to fast electron transfer, excellent mechanical and thermal stability and excellent electrocatalytic activity. The high density of edge plane defect sites on OMC may provide many favorable sites for electron transfer to enable the OMCs as a promising nanostructure for electrode modification [17]. These properties have been intelligently combined to selected redox processes to design novel sensors and biosensors. OMCs with various structures, designated as CMK-1~5 (Carbon Molecular sieves from Korea Advanced Institute of Science and Technology), have been synthesized by carbonization of sucrose, furfuryl alcohol or other suitable carbon sources inside silica or aluminosilicate mesopores that are interconnected into three-dimensional networks [18]. In a specific case of CMK-1, the synthesis using MCM-48 (Mobil composition of matter no. 48) undergoes the structural transformation from cubic $Ia3d$ to tetragonal $I4_132$ or lower due to the displacement. [12].

The direct electro-oxidation of CAR at different electrodes such as GCE [19-21], platinum electrode in acetonitrile solution [22] and copper-oxide nanoparticle modified carbon paste electrode [23] has been investigated. However, it was reported that the use of an unmodified GCE suffers from sluggish electron transfer and fouling of surface which result in poor sensitivity, narrow linear range and selectivity. Other method such as high-performance liquid chromatography with electrochemical detection[24] has been proposed for the analyses of CAR. However, this method require time consuming manipulation step, sophisticated instrument and special training.

In our work, an OMC, CMK-1, modified GCE was successfully fabricated by coating OMC onto GCE after preparation of CMK-1 using mesoporous silica materials MCM-48 as the template and sucrose as the carbon source, then this electrode was employed to investigate the electrochemical behaviors and quantification of carvedilol by voltammetry. As an evaluation of this electrode, serum, tablet and human urine, were selected and satisfying results were obtained.
To the best of our knowledge, this is the first report on CAR determination using OMCs/GCE.

2. Experimental

2.1. Apparatus

An Autolab electrochemical analyzer, Model PGSTAT 302 N potentiostat/galvanostat (Eco-Chemie, The Netherlands), and a three electrode electrochemical cell: an Ag/AgCl/KCl (3 M) reference electrode (Metrohm) and a platinum wire as a counter electrode were used for electrochemical studies. The applied working electrode in this study was a GCE or OMCs/GCE. The Brunauer–Emmet–Teller (BET) specific surface areas and Barrett–Joyner–Halenda (BJH) pore size distribution of the samples were determined by adsorption–desorption of nitrogen at liquid nitrogen temperature, using a Series BEL SORP 18. The X-ray powder diffraction (XRD) was carried out on a Bruker D8Advance X-ray diffractometer using nickel

filtered Cu Kα radiation at 40 kV and 20 mA. Scanning electron microscope (SEM) studies were performed on Philips, XL30, SE detector.

2.2. Chemicals

CAR and other pharmaceuticals were kind gifts from Dr. Amidi (School of Pharmacy, Shahid Beheshti University of Medical Sciences, Tehran, Iran) and used without further purification. All other reagents were of analytical grade and used without further purification. Phosphate buffer, Britton–Robinson (B-R) universal buffer (0.04 M boric acid, 0.04 M acetic acid and 0.04 M phosphoric acid), acetate buffer and KNO_3 solution were prepared in deionized water and were tested as the supporting electrolytes.

2.3. Preparation of MCM-48

MCM-48 was prepared as our previous report [25]. In brief, cetyltrimethylammonium bromide (CTAB) (2.4 g, 6.6 mmol) was dissolved in 50 mL deionized water. To this, 50 mL technical grade ethanol (0.87 mol) and 12 mL of aqueous ammonia (32 wt. %, 0.20 mmol) were added. The solution was stirred for 10 min, after which tetraethylorthosilicate (TEOS) (3.4 g, 16 mmol) was added. After stirring for 2 h at room temperature, the resulting solid was recovered by filtration, washed with deionized water and dried in air at ambient temperature. The template was removed by calcination at 550°C for 6 h.

2.4. Preparation of CMK-1

1g MCM-48 was added to 5mL aqueous solution containing 1.25g (3.65mmol) sucrose and 0.14g (1.42mmol) of H_2SO_4 (98%). The resulting mixture was heated in an oven at 100°C for 6h and then 160°C for another 6h. In order to obtain fully polymerized sucrose inside the pores of the MCM-48 template, 5mL aqueous solution containing 0.75g (2.19mmol) sucrose and 0.08g (0.79mmol) of H_2SO_4 were added again and the mixture was subjected to the thermal treatment described above one more time. Then, it was carbonized under N_2 gas flow at 900°C for 6h with a heating rate of 5°C min^{-1}. Finally, the resulting solid was washed with 1M NaOH solution (50 vol.% ethanol–50 vol.% H_2O) twice to remove the silica template, filtered, washed with ethanol until pH 7, and dried at 100°C for 4h. Thus, mesoporous carbon CMK-1 was obtained as OMC [26].

2.5. Preparation of real samples

Ten tablets containing 25mg CAR were weighed and finely powdered in a small dish. The equivalent of 25mg CAR was weighed and transferred in a 100mL volumetric flask, mixed with methanol (50 mL) and sonicated for 20 min to ensure that tablets were dissolved completely and centrifuged for 15min. The supernatant was separated and the residue was treated with a fresh portion of 10 mL methanol. The two portions were combined in a 100mL volumetric flask and diluted to the mark with methanol and filtered through Millipore membranes of 0.45 mm pore size. Next, 10 mL of the filtered solution was transferred to a flask and increased in volume (100mL) with methanol. Analyzed solutions were prepared by taking aliquots of this solution and diluting with the selected supporting

electrolyte. Voltammograms were recorded in a similar way as for standard solutions of CAR.

Drug-free human serum was prepared from heparinized whole-blood samples collected from healthy volunteers and stored at 20°C until use after gentle thawing. Due to possibility of protein-bonding for CAR and reducing the recoveries processes, it is necessary to have some treatments with plasma before analysis. Acetonitrile was used as a serum precipitating agent and the mixture was centrifuged at 6000 rpm for 30 min at 4°C. Then, the supernatant was filtered through a cellulose acetate filter (0.2 μm pore size, Advantec MFS, CA) and then spiked with exogenous CAR. No extraction steps other than centrifugal protein separation were required prior to assay for the drug.

Fresh human urine samples were obtained from volunteer who had not taken CAR and stored in a refrigerator at 4°C immediately after collection. The matrices of 2mL urine were precipitated with 2 mL of acetonitrile and 2 mL of B-R buffer solution (pH 2 and 8), and mixed. The samples were centrifuged (6000 rpm) for 30 min. Then the supernatant was filtered through a cellulose acetate filter (0.2 μm pore size, Advantec MFS, CA) and then spiked with exogenous CAR. No extraction steps other than centrifugal protein separation were required prior to assay for the drug

2.6. Modification of electrodes

The bare GCE (3 mm diameter) was polished sequentially with metallographic abrasive paper (No. 6), 0.3 and 0.05 μm alumina to obtain a mirror finish, and then sonicated with methanol and water for about 2 min, respectively. After that, the GCE was rinsed thoroughly with water and dried with nitrogen steam for the following experiment use.

The obtained CMK-1 (5 mg) was dispersed in 10 mL N,N-dimethyl formamide and the mixture was sonicated for 30 min to obtain a homogeneous black suspension. Then, 5 μL of the obtained suspension was dropped on the GCE surface and allowed to dry for about 15 min under an infrared lamp to obtain CMK-1/GCE.

3. Results and discussion

3.1. CMK-1/GCE characterization

Fig. 1a shows the powder X-ray diffraction patterns of silica MCM-48 and CMK-1. Both samples exhibit a strong (211) diffraction peak at ~2.35° . As can be seen, the XRD pattern of CMK-1 sample is similar to that of MCM-48, indicating that CMK-1 is a true replica of the mesoporous silica MCM-48.

The SEM images of MCM-48 and CMK-1 are shown in Fig. 1b and 1c respectively. MCM-48 is agglomerations of small spherical regular particles. As can be seen, there is no significant difference between morphologies of CMK-1 and MCM-48 which indicates that CMK-1 is a true replica of the mesoporous silica MCM-48.

The BET specific surface areas, the pore volumes and the pore sizes of MCM-48 and CMK-1, samples were calculated using BET and BJH methods (Table 1). The nitrogen sorption isotherms for these samples are shown in Fig. 2. As can be seen, these isotherms are similar to isotherms of type IV, according to the IUPAC nomenclature, which are the typical characteristics of mesoporous materials . It is seen that MCM-48 has a high BET surface area (1673 m^2 g^{-1}), a large pore volume (0.89 cm^3 g^{-1}) and pore size (2.14 nm), indicative of its potential application as a proper hard template material. Also, CMK-1 shows a high BET surface area (809 m^2 g^{-1}), a large pore volume (0.63 cm^3 g^{-1}) and pore size (3.1 nm) which indicates that CMK-1 is a true replica of the mesoporous silica MCM-48.

The effective surface area of the CMK-1/GCE was estimated from the cyclic voltammograms of a 0.5 mM $K_3[Fe(CN)_6]$/0.1 M KCl solution at various scan rates. Cyclic voltammograms obtained at the CMK-1 modified GCE and a bare GCE were shown in Fig. 3. The peak separations are found to be 82 mV and 107 mV at CMK-1/GCE (curve a) and the bare GCE (curve b), respectively. As ΔEp is a function of the rate of electron transfer, the lower ΔEp indicates a higher electron transfer rate. It can be deduced that a higher electron transfer rate was occurred at CMK-1 modified GCE compared with that of bare GCE. For a reversible process, the Randles– Sevcik formula was used [27].

$$Ip = 2.69 * 10^5 n^{3/2} ACD^{1/2}v^{1/2}$$

where Ip refers to the anodic peak current, n the number of electrons transferred, A the surface area of the electrode, D the diffusion coefficient, C the concentration of $K_3[Fe(CN)_6]$, and v is the scan rate. For 0.5 mM $K_3[Fe(CN)_6]$ in the 0.1 M KNO_3 electrolyte: n = 1 and D = 7.6×10^{-6} cm^2 s^{-1} [28], then from the slope of Ip versus v$^{1/2}$, the effective area was calculated to be 0.0726cm^2 which is higher than that of GCE (0.0593 cm^2).

Comparison of OMC and other carbon materials such as carbon nanotube (CNT) and glassy carbon electrode (GCE) shows that the electrochemical response currents at OMC modified electrodes are higher than that of the GCE and CNT modified electrode[16, 29]. It has been shown that the electron transfer resistance of OMC is much lower than that of CNT [30] suggesting that OMC can form good electron pathway between the electrode and electrolyte. Recent works showed that the apparent electrode surface area is higher than that of CNT [31]. This large value of the electrode area is attributed to the higher surface to volume ratio and roughness factors of OMC [31]. The apparent capacitance of OMC was calculated being a value of 197 μF cm^{-2} by Zhu et al [32], which is much lower than that of CNT. This is very interesting because a lower capacitance results in a lower charging current. Therefore based on the above evidence, CMK-1 can be used as an appropriate modifier with regular structure and a very high surface area for electrode modification.

3.2. Electrochemical impedance spectroscopy (EIS) studies

EIS is an effective method to probe the interfacial properties of the modified electrode and often used for understanding chemical transformations and processes associated with the conductive supports [9]. Fig. 4 exhibits the Nyquist plots of the GCE and CMK-1/GCE. To obtain the detailed information of EIS, a simple equivalent circuit model was used to fit the results (inset). In this circuit, R_s, R_{dl} and R_{et} represent solution resistance, a capacitance for the double-
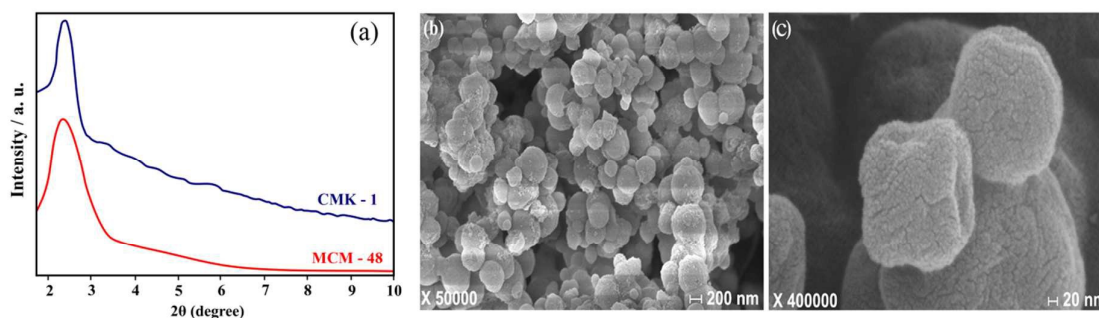
Fig. 1. (a) Comparison of XRD patterns of MCM-48 and CMK-1, SEM images of (b) MCM-48 and (c) CMK-1.

Table 1: Physicochemical properties of mesoporous silica MCM-48 and mesoporous carbon CMK-1, obtained from N_2 adsorption.

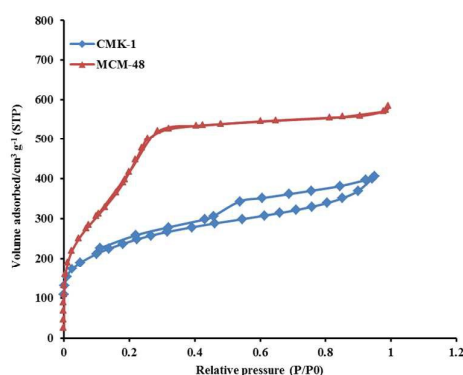| sample	BET (m^2g^{-1})	V_p (cm^3g^{-1})	BJH (nm)
MCM-48	1673	0.89	2.14
CMK-1	809	0.63	3.1

Fig. 2. N2 adsorption–desorption isotherms of MCM-48 and CMK-1
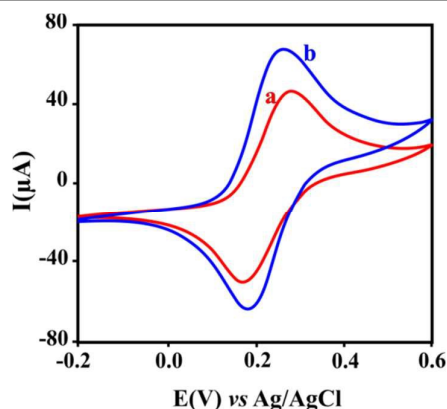

Fig. 3. CVs of 5 mM $K_3Fe(CN)_6$ 0.1 M KCl at GCE (curve a) and CMK-1/GCE (curve b). Scan rate: 100 mV/s.

layer and electron transfer resistance, respectively. W is a finite-length Warburg short-circuit term coupled to R_{et}, which accounts for the Nernstian diffusion. R_{et} at the electrode surface is equal to the semicircle diameter, which can be used to describe the interface properties of the electrode. The R_{et} of the electrode at different stages altered with the modification, which was measured at a formal potential of 0.2 V versus Ag/AgCl in $[Fe(CN_6)]^{3-/4-}$ as the redox probe. The GCE showed a high R_{et} value of 240Ω. After the GCE was modified with CMK-1 the R_{et} was decreased to the value of 36 Ω, revealing the satisfactory electrical conductivity with the introduction of CMK-1.

3.3. Electrochemical behaviors of CAR at CMK-1/GCE

Cyclic voltammograms (CV) measurements were carried out to examine the electrochemical behavior of CAR on CMK-1/GCE employing various supporting electrolytes with different pH values, such as Britton-Robinson (pH 2.0-12.0), phosphate (pH 2.0-8.0) and acetate (pH 3.5–5.5) buffer solutions. B-R buffer solutions yielded lower background currents (compared to other buffer solutions) with high peak currents and repeatable signals, thus it was chosen as supporting electrolyte for all subsequent electrochemical measurements. Fig. 5 shows CVs of 20 µmol L^{-1} CAR at various electrodes in 100 mVs^{-1} scan rate. On the CMK-1/GCE two anodic peaks were observed. During the anodic scan one distinct well-defined and high oxidation peak at 0.65 V (P_1) is manifested beside a second weak signal at 0.86 V (P_2) at pH=8.0 (Fig. 5I). Also, at pH=2.0, these peaks can be seen at 0.88 V (P_1) and +1.1 V (P_2) which P_2 current is higher than P_1 (Fig. 5II). No corresponding reduction peak of CAR is observed in the reverse scan, which indicates that the electrochemical behavior of CAR at the CMK-1/GCE is an irreversible and sluggish process. Insets of Fig. 5 shows CV responses of various electrodes were obtained in the B–R buffer of pH 8.0 and 2.0 for P_1 and P_2, respectively. It can be distinctly seen that the oxidation of CAR at the bare GCE requires a large over potential. Compared with that of the bare GCE, the oxidation peak current of CAR increases significantly and the oxidation peak potential shifts negatively at the CMK-1/GCE. The obviously increased peak current and the decrease in the anodic over potential for CAR clearly demonstrate that CMK-1/GCE exhibits a good electrochemical response and

faster electron transfer kinetics for the oxidation of CAR. This is most likely to be attributed to the large surface area of CMK-1 and a large number of edge plane defect sites at the surface of the CMK-1/GCE, which may provide many favorable sites for electron transfer to molecules.

3.4. Effect of pH on the peak potentials and peak currents

Generally, the nature and pH value of supporting electrolyte is a significant factor that affects the electrochemical behavior and sensitivity of the determination of various biologically active compounds. CAR at the surface of CMK-1/GCE shows two peaks. Various parameters affect the peak potentials and peak currents. Optimal conditions for obtaining high peak current and well defined peak shape for the two are different. Since the potential of these peaks are far from each other. In some cases, one compound is interference for first oxidation peak, but second oxidation peak of CAR is interference free and vice versa. Therefore, according to the type of samples and interferences, one of them can be used for analysis.

It was found that phosphate and acetate buffer solutions yielded higher background currents (compared to B-R buffer solutions) with less repeatable signals. Nevertheless, in B-R buffer solutions, the peak current of CAR presented highest magnitude, lowest background current and best repeatability. Thus it was chosen as supporting electrolyte for all subsequent electrochemical measurements. The influence of pH on both peak potentials (Ep1 and Ep2) and the corresponding peak currents (Ip1 and Ip2) of 10 μmol L^{-1} CAR was systematically studied by DPV in the pH range of 2–12 using B-R buffer solutions (Fig. 6a). It was found that both peak potentials of CAR shifted towards less positive potential values with the increase of pH of the supporting electrolyte as depicted in the Fig. 6b and c. It is an indubitable fact that protons represent an important participator in the oxidation process of CAR on the CMK-1/GCE electrode. These dependences are linear over the whole studied pH range and two linear plots obtained; one from pH 2.0 to 8.0 and the second from pH 8.0 to 12.0. They can be described by the following equations (Eqs. (1) to (4)):

$$E = -0.037\ pH + 0.951\ (R^2 = 0.996)\ for\ P1\ (pH\ 2.0\ to\ 8.0) \quad (1)$$
$$E = -0.068\ pH + 1.21\ (R^2 = 0.988)\ for\ P1\ (pH\ 8.0\ to\ 12.0) \quad (2)$$
$$E = -0.040\ pH + 1.167\ (R^2 = 0.983)\ for\ P2\ (pH\ 2.0\ to\ 8.0) \quad (3)$$
$$E = -0.026\ pH + 1.071\ (R^2 = 0.985)\ for\ P2\ (pH\ 8.0\ to\ 12.0) \quad (4)$$

Also, influences of the pH on the peak current are shown in Fig. 6d. The first and second peak currents of CAR were maximum in pH 8.0 and 2.0, respectively.

3.5. Effect of scan rate on the peak currents and peak potentials

The effect of the scan rate (v) on both peak currents (I$_{p1}$ and I$_{p2}$) was investigated by CV in order to characterize the nature of the kinetic control of the reaction at CMK-1/GCE (rate-determining step) (Fig. 7). The current responses for both oxidation peaks of CAR increased linearly with the square root of the scan rate within the range of 50-400 mV s^{-1} (with very similar slope values, Fig. 7a$_3$ and b$_3$), suggesting that at a sufficiently positive potential, the diffusion is the rate-
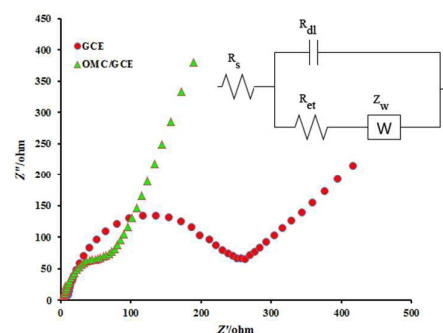

Fig. 4. Nyquist plots for various prepared electrodes in the 1.0 mmol L^{-1} [Fe(CN)$_6$]$^{3-/4-}$ and 0.1 mol L^{-1} KCl.
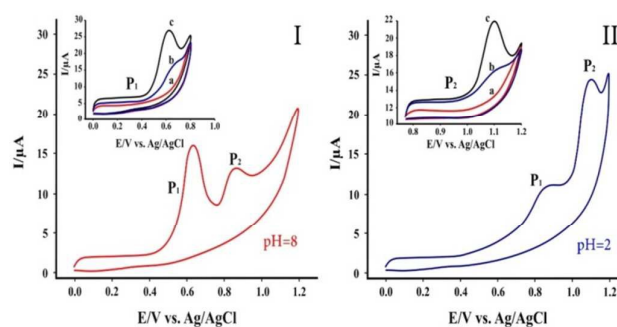

Fig. 5. CVs for 20.0 μM CAR in B-R buffer solution (I) pH= 8 and (II) pH=2 on the surface of CMK-1/GCE. Insets show CVs for 20.0 μM CAR at (a) CMK-1/GCE in absence of analyte, (b) GCE (c) CMK-1/GCE.

determining step in the oxidation process and adsorption and/or specific interactions on CMK-1/GCE electrode surface are negligible. The linear dependences can be expressed by the following equations (Eqs. (5) and (6)):

$$I_p\ (μA) = 0.9079 υ^{1/2}\ (mV\ s^{-1}) + 1.230\ (R^2 = 0.995)\ (For\ P_1) \quad (5)$$

$$I_p\ (μA) = 0.611\ υ^{1/2}\ (mV\ s^{-1}) + 0.391\ (R^2 = 0.995)\ (For\ P_2) \quad (6)$$

A linear relationship was observed between log I$_{pa}$ and log v, corresponding to the following equation: The slope values of 0.44 and 0.46 were comparable with the theoretically expected value of 0.5 for a purely diffusion controlled current [33].

$$log\ I_{pa}(μA) = 0.440\ log\ v + 0.137;\ (R^2 = 0.991) \quad (For\ P_1) \quad (7)$$
$$log\ I_{pa}(μA) = 0.459\ log\ v - 0.099;\ (R^2 = 0.992) \quad (For\ P_2) \quad (8)$$

It confirms that the electro-oxidation of CAR is diffusion controlled.

3.6. Analytical performance of the sensor for CAR measurements

The main objective of this study was to develop a novel modified electrode for determination of CAR. Differential pulse voltammetry (DPV), which has lower charging current contribution to the background current and a much higher current sensitivity than CV was used to estimate the linear
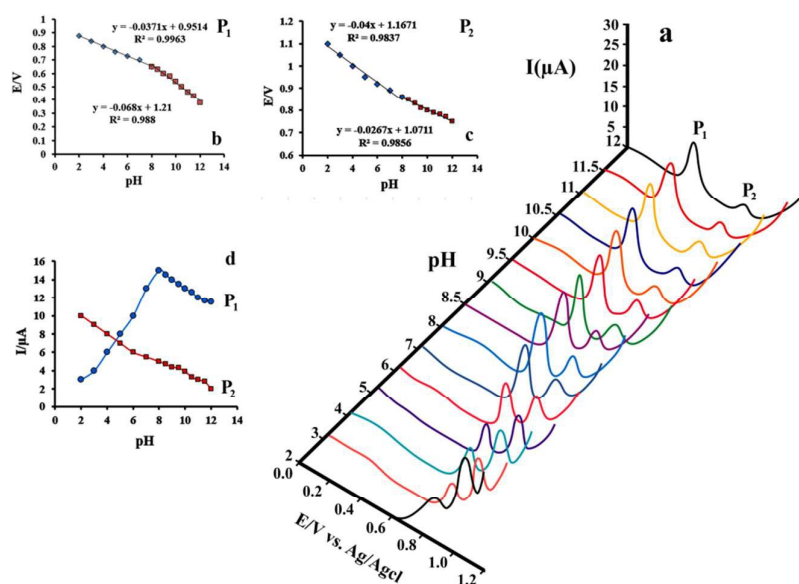
Fig. 6. (a) DPVs for CMK-1/GCE in 10 µmol L^{-1} CAR at various pHs (pH 2, 3, 4, 5, 6, 7, 8, 8.5, 9, 9.5, 10, 10.5, 11, 11.5, 12). (b) Effects of pH on the peak potentials of P$_1$. (c) Effects of pH on the peak potentials of P$_2$ (d) Effect of pH on the peak current of P$_1$ and P$_2$

range of CAR and the lower limit of detection. The effect of increasing the CAR concentration on the voltammetric responses is presented in Fig. 8 (in the range of 0.1 to 23.0 µmol L^{-1} for the first peak and 0.12 to 18.0 µmol L^{-1} for the second peak). Insets of Fig. 8 clearly show that the plots of the peak current versus the CAR concentration are linear with slopes of 1.441 and 1.108, respectively. Comparison of the sensitivities of the two linear plots indicates a decrease of the sensitivity in the second linear range of the calibration plot for P$_2$. It is well known that with increase of an analyte concentration in the solution, the thickness of diffusion layer and thus mass transfer limitation are reduced. In other words, decrease of the sensitivity (slope) of calibration plot is likely due to the electron transfer kinetic limitation in the interactions among the analyte, CAR, and the modifier. The practical detection limit ($3s_b$/m) is obtained 0.034, 0.044 µmol L^{-1} for first and second anodic peaks of CAR, respectively.

The average voltammetric peak currents for the first peak and the precision estimated in terms of the Relative Standard Deviation (RSD) for 10 replicates (N = 10) of 1 µmol L^{-1} of CAR at CMK-1/GCE were 0.75 µA and 2.1%, respectively. For the second peak, voltammetric peak current and the precision of 1 µmol L^{-1} of CAR were 0.68 µA and 2.3%, respectively. The RSD values indicate that the modified electrode is stable and does not undergo surface fouling during voltammetric measurements. This also demonstrates the fact that the results obtained at the sensor are repeatable in analytical applications. In Table 2, some of the analytical characteristics of the developed method were compared with those previously reported by others. As it can be seen, the capabilities of the proposed sensor are superior in most cases than the others.

3.7. Interferences study

Selectivity and applicability of the proposed method was also evaluated by investigating the effect of some common species that often accompany CAR in real samples such as blood and urine. This study was done for a solution of 1 µmol L^{-1} of CAR and the tolerance limit is defined as the molar ratio of the foreign species to CAR that causing 5% relative error for CAR determination.

The interference study was conducted by placing the CMK-1/GCE into a solution containing target analytes at optimum conditions. It was found that 800-fold of K$^+$, Na$^+$, NH$_4^+$, Ca^{2+}, Mg^{2+}, SCN$^-$, NO$_3^-$, SCN$^-$ have no influence on the signal of CAR. 250-fold excess of glycine and valine, 100-fold excess of ascorbic acid and 50-fold excess of acetaminophen had no effect on the signals of CAR. Lactose, glucose and sucrose showed no changes in the signals until 300-fold excess was used. These results suggested that the determination of CAR in pharmaceutical formulations and biological samples at CMK-1/GCE was not significantly affected by the most common interfering species.

3.8. Application

To evaluate the applicability of proposed method, the recovery of CAR was determined in serum, urine and pharmaceutical samples. The standard addition method was used for the analysis of prepared samples. The data given in Table 3 shows the satisfactory results. As shown in Table 3, the recoveries for the determination of CAR were from 96.6% to 103.3% and the RSD was below 3% (N=5), which indicated that the presented method could be efficient and reliable for the determination of CAR in routine analysis.

3.9. Reproducibility and stability

The reproducibility and stability of the CMK-1/GCE were carried out for 2 µmol L^{-1} CAR. The relative standard deviation
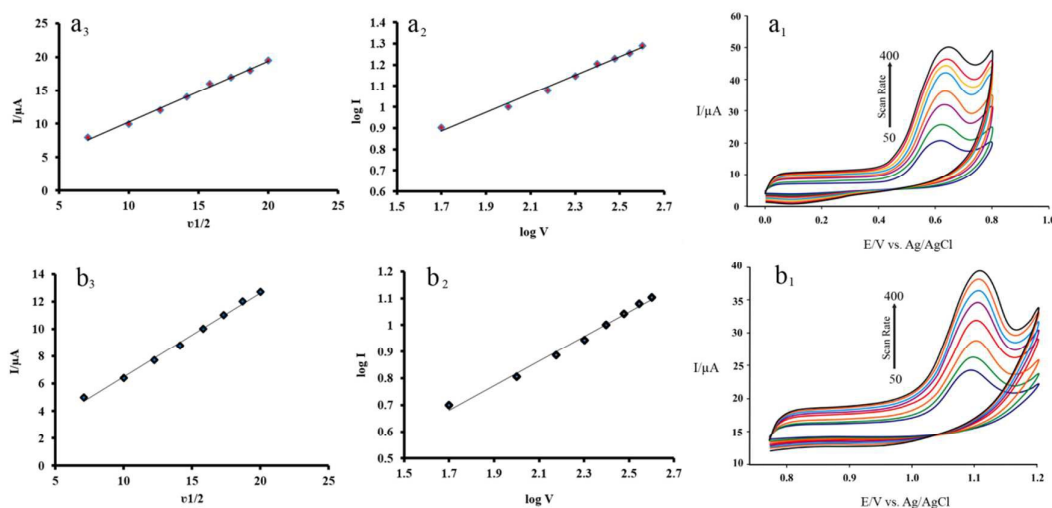
Fig. 7. Cyclic voltammograms of CMK-1/GCE containing 20 µmol L^{-1} of CAR (a$_1$) in B-R Buffer (pH 8) for P$_1$ with scan rate ranging from a to f as 50, 100, 150, 200, 250, 300, 350, 400 mV s^{-1} , respectively. and (b$_1$)) in B-R Buffer (pH 2) for P$_2$ with scan rate ranging from a to f as 50, 100, 150, 200, 250, 300, 350 and 400 mV s^{-1}. linear relationship of the anodic peak current versus square root of the scan rate (υ ½) (a$_2$) P$_1$ and (b$_2$) P$_2$. linear relationship of the Log (I$_p$) versus Log (☐) (a$_3$) P$_1$ and (b$_3$) P$_2$.
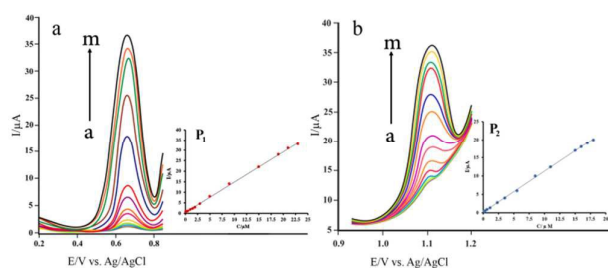

Fig. 8. (A) DPVs of CAR at CMK-1/GCE in B-R buffer solution (a) pH 8 for P$_1$, concentrations (from a to m): 0.1, 0.15, 0.5, 1, 1.5, 2, 3, 5, 9, 15,19, 21 and 23 µmolL^{-1} . (b) pH 2 for P$_2$, concentrations (from a to m): 0.12, 0.3, 0.6, 1.1, 2.3, 3.5, 5.5, 8.5, 11, 15, 16, 17 and 18 µmolL^{-1} .

Table 2: Comparison of some characteristics of the proposed electrode with those previously reported

Electrode	Range (µM)	LOD (µM)	Method	Ref
GCE	0.2-20	0.0020	AdSDPV	19
		0.0023	AdSSWV	
n-MCPEs	5-37	3.01	DPV	23
GCE	0.61-25	0.25	DPV	21
GCE	6.2-55.3	2.1	DPV	20
Pt	12.3-98.4	3.2	LSV	22
CMK-1-GCE	0.10-23.00	0.034	DPV	This work

(RSD) was 2.46% for ten measurements with the same electrode and the RSD of 3.66% was obtained for ten different

modified electrodes with the same test solution. After one month storage in lab ambient, the current response for 2 µmol L^{-1} CAR remained 95% of the initial value. The results indicated the excellent reproducibility and stability of the presented modified electrode for the detection of CAR.

4. conclusion

In this work, we present an advanced electrochemical sensing platform based on ordered mesoporous carbon. CMK-1 was synthesized by using MCM-48 as the template and sucrose as the carbon source and used for electrochemical determination of CAR as a modifier in sensing layer. Owning to the unique properties of CMK-1 such as high surface area, large pore volume, etc., the CMK-1 modified electrode exhibited more favorable electron transfer kinetics than bare GCE and enhanced the electrochemical response of CAR. The CMK-1/GCE showed high sensitivity and excellent detection limit (0.034 µmol L^{-1}) in a wide determination range (0.1-20 µmol L^{-1}) by DPVs method. Furthermore, the proposed modified electrode was applied for the determination of CAR in tablet, serum and urine samples. The satisfied results indicated that CMK-1 will be a promising electrode modifier for the measurement of CAR in real samples. Therefore, a simple, sensitive, reproducible and cost-effective sensor was proposed for the fast direct measurement of CAR.

5. Acknowledgments

Table 3: Results for CAR determination (µmol L^{-1}) in various real samples obtained by the proposed method under the optimum conditions

sample	pH= 2			pH=8		
	Added	Found	Recovery (%)	Added	Found	Recovery (%)
Serum	0.0	-	-	0.0	-	-
	0.30	0.29	96.6	0.3	0.31	103.3
	2.0	1.98	99.0	2	2.05	102.5
Urine	0.0	-	-	0.0	-	-
	0.5	0.49	98.0	0.5	0.49	98.0
	3.0	3.05	101.6	3	3.09	103
Tablet	0.0	0.63	-	0.0	0.59	-
	0.8	1.45	102.5	0.8	1.38	98.7
	2.0	2.62	99.5	2	2.54	97.5

References

1. K. Nakamura, K. Kusano, Y. Nakamura, M. Kakishita, K. Ohta, S. Nagase, M. Yamamoto, K. Miyaji, H. Saito and H. Morita, *Circulation*, 2002, 105, 2867-2871.

2. M. L. Kukin, J. Kalman, R. H. Charney, D. K. Levy, C. Buchholz-Varley, O. N. Ocampo and C. Eng, *Circulation*, 1999, 99, 2645-651.

3. P. A. Poole-Wilson, J. G. Cleland, A. Di Lenarda, P. Hanrath, M. Komajda, M. Metra, W. J. Remme, K. Swedberg and C. Torp-Pedersen, *European Journal of Heart Failure*, 2002, 4, 321-329.

4. D. W. Graff, K. M. Williamson, J. A. Pieper, S. W. Carson, K. F. Adams, W. E. Cascio and J. H. Patterson, *The Journal of Clinical Pharmacology*, 2001, 41, 97-106.

5. K. FUKUMOTO, T. KOBAYASHI, K. KOMAMURA, S. KAMAKURA, M. KITAKAZE and K. UENO, *Drug metabolism and pharmacokinetics*, 2005, 20, 423-427.

6. S. M. Stout, J. Nielsen, B. E. Bleske, M. Shea, R. Brook, K. Kerber and L. S. Welage, *Journal of cardiovascular pharmacology and therapeutics*, 2010, 15, 373-379.

7. H. Beitollahi, S. Tajik and P. Biparva, *Measurement*, 2014, 56, 170-177.

8. H. Bagheri, S. M. Arab, H. Khoshsafar and A. Afkhami, *New Journal of Chemistry*, 2015, 39, 3875-3881.

9. A. Afkhami, H. Khoshsafar, H. Bagheri and T. Madrakian, *Analytica chimica acta*, 2014, 831, 50-59.

10. N. Lavanya, E. Fazio, F. Neri, A. Bonavita, S. G. Leonardi, G. Neri and C. Sekar, *Sensors and Actuators B: Chemical*, 2015, 221, 1412-1422.

11. Nhi S. Nguyen, G. Das and Hyon H. Yoon, *Biosensors and Bioelectronics*, 2016, 77, 372-377.

12. R. Ryoo, S. H. Joo and S. Jun, *The Journal of Physical Chemistry B*, 1999, 103, 7743-7746.

13. H. Yang, B. Lu, B. Qi and L. Guo, *Journal of Electroanalytical Chemistry*, 2011, 660, 2-7.

14. J. Yu, W. Du, F. Zhao and B. Zeng, *Electrochimica Acta*, 2009, 54, 984-988.

15. J. Zang, C. X. Guo, F. Hu, L. Yu and C. M. Li, *Analytica chimica acta*, 2011, 683, 187-191.

16. J. C. Ndamanisha and L.-p. Guo, *Analytica chimica acta*, 2012, 747, 19-28.

17. A. Walcarius, *TrAC Trends in Analytical Chemistry*, 2012, 38, 79-97.

18. R. Ryoo, S. Joo, S. Jun, T. Tsubakiyama and O. Terasaki, *Stud Surf Sci Catal*, 2001, 135, e8.

19. B. Dogan and S. A. Ozkan, *Electroanalysis*, 2005, 17, 2074-2083.

20. I. Baranowska, M. Koper and P. Markowski, *Che m Anal*, 2008, 53, 967-981.

21. A. Radi and T. Elmogy, *Il Farmaco*, 2005, 60, 43-46.

22. B. Yilmaz and D. Ekinci, *Reviews in Analytical Chemistry*, 2011, 30, 187-193.

23. N. Shadjou, M. Hasanzadeh, L. Saghatforoush, R. Mehdizadeh and A. Jouyban, *Electrochimica Acta*, 2011, 58, 336-347.

24. M. Machida, M. Watanabe, S. Takechi, S. Kakinoki and A. Nomura, *Journal of Chromatography B*, 2003, **798**, 187-191.

25. R. J. Kalbasi and N. Mosaddegh, *catalysis communications*, 2011, 12, 1231-1237.

26. R. J. Kalbasi, N. Mosaddegh and A. Abbaspourrad, *Applied Catalysis A: General*, 2012, 423, 78-90.

27. A. J. Bard and L. R. Faulkner, *Electrochemical Methods, 2nd ed.; Wiley: New York*, 2001.

28. B. Rezaei and Z. M. Zare, *Analytical Letters*, 2008, 41, 2267-2286.

29. M. Zhou, L. Shang, B. Li, L. Huang and S. Dong, *Electrochemistry communications*, 2008, 10, 859-863.

30. D. Feng, Y. Lv, Z. Wu, Y. Dou, L. Han, Z. Sun, Y. Xia, G. Zheng and D. Zhao, *Journal of the American Chemical Society*, 2011, 133, 15148-15156.

31. J. Bai, J. C. Ndamanisha, L. Liu, L. Yang and L. Guo, *Journal of Solid State Electrochemistry*, 2010, 14, 2251-2256.

32. L. Zhu, C. Tian, D. Yang, X. Jiang and R. Yang, *Electroanalysis*, 2008, 20, 2518-2525.

33. A. A. Rafati, A. Afraz, A. Hajian and P. Assari, *Microchimica Acta*, 2014, 181, 1999-2008.